ASSESSMENT OF TOXIC METAL IONS REMOVAL BY NOVEL NANOPOROUS BIO-CHARS

Ivanka Stoycheva[1], Boyko Tsyntsarski[1], Bilyana Petrova[1], Angelina Kosateva[1], Nartzislav Petrov[2], Georgi Tirolski[1], Maria Argirova[1], Pavlina Dolashka[2], Teodor Sandu[3], Andrei Sarbu[3]

[1]*Institute of Organic Chemistry with Centre of Phytochemistry Bulgarian Academy of Sciences, Acad. G. Bonchev St., Bl. 9, Sofia 1113, Bulgaria; ivanka.stoycheva@orgchm.bas.bg (I.S.); boyko.tsyntsarski@orgchm.bas.bg (B.T.); bilyana.petrova@orgchm.bas.bg (B.P.); angelina.kosateva@orgchm.bas.bg (A.K.); Georgi.Tirolski@orgchm.bas.bg (G.T.); Maria.Argirova@orgchm.bas.bg (M.A.)*

[2]*Center of Competence "Clean Technologies for Sustainable Environment - Water, Waste, Energy for Circular economy", 15 Tsar, Osvoboditel Blvd., Sofia 1000, Bulgaria nartzi@abv.bg (N.P.); pda54@abv.bg (P.D.)*

[3]*National Research - Developent Institute for Chemistry and Petrochemistry INCDCP-ICECHIM, Spl. Independentei 202, sector 6, Bucharest, Romania sanduteodor85@gmail.com (T.S.); andr.sarbu@gmail.bg*

Received 28 July 2025
Accepted 05 October 2025
DOI: 10.59957/jctm.v61.i2.2026.7

ABSTRACT

Novel nanoporous bio-chars with well-developed mesoporous structure, derived from juice industry residues, are obtained by applying new energy-saving treatment method. Using a precursor with a significantly high content of cellulose, hemicellulose, and lignin (cherry stones) results in the formation of carbonaceous material with micro- and mesopores, whereas a raw material with a higher content of lipids and lignin (dried aronia fruit residue) produces carbon with narrow microporosity. The cadmium adsorption capacity values for activated carbon from cherry stones and aronia residue are 93 and 70 mg g^{-1}, and mercury adsorption capacities are 83 and 104 mg g^{-1}, respectively. The characteristics of the obtained nanoporous bio-chars indicate that they are suitable for the removal of highly toxic metal ions from wastewater.

Keywords: toxic heavy metals, cadmium, mercury, adsorption, biomass, bio-char.

INTRODUCTION

Cadmium, lead and mercury are among the most toxic heavy metals. The main sources of cadmium pollution are mining industry, metallurgy, metal coatings, Cd-Ni batteries, phosphate fertilizers, pigments, stabilizers, ceramics, photography, textile printing, etc. [1 - 5]. Commercial activated carbon is widely used for efficient removal of heavy metals from waters - this is determined by its high specific surface area and high adsorption capacity towards metal ions, however the relatively high cost and sludge formation sometimes can limit the application of carbon adsorbents [6 - 9]. Carbon materials have high affinity towards cadmium ions [10 - 12], however other materials are also used for cadmium removal - clay minerals [13, 14], oxides [15], membranes [16, 17], chelating resins [18], etc.

Mercury is one of the most toxic elements found in the environment. Once mercury enters the food chain, high degree of accumulation of mercury compounds can be detected in human and animals. Mercury has adverse effects on the central nervous system, pulmonary and

kidney functions, and causes damage to chromosomes. The limit for Hg (II) discharge into inland surface waters is 10 μg L^{-1}, and in drinking water - 1 μg L^{-1}. The drinking water limit for Hg^{2+} established by USEPA is 2 μg L^{-1} [19].

The lethal oral doses for humans and allowable concentrations in drinking water of Cd and Hg are presented in Table 1.

The major sources of mercury pollution in the aquatic environment are industries such as chloralkaline, pulp paper, paint, rubber processing, oil refining, electrical and fertilizer production [20]. Numerous methods are available for removal of mercury, including chemical precipitation, coagulation, reverse osmosis, ion exchange, chelating, and adsorption [21, 22].

As the demands for a sustainable society grows, the biomass, which is a carbon-neutral resource, is recognized as a very important material in the circular economy. Agricultural by-products are very promising raw materials to produce activated carbon due to their low-cost and availability [1, 2].

Utilization of waste biomass from various industries is very important, and it can be performed by thermochemical processes, such as pyrolysis and gasification, or by different fermentation technologies. Pyrolysis is a process of thermal treatment of the raw material in an inert atmosphere, whereas gaseous, liquid and solid products are released [23]. All these products can find different applications. The gas and liquid products can be utilized to generate energy, for production of valuable chemicals, and as raw materials they can be used for synthesizing carbon materials. The solid products, without or with additional processing, can be converted into porous carbons with a wide range of applications. Thermal treatment often eliminates moisture and volatiles from biomass, and the resultant solid char has a different composition and pore structure than the primary precursor materials, as well as high surface reactivity and area [24]. Any organic material with high carbon and low ash content can be successfully applied as a raw material to produce porous carbon [25].

Among many other suitable materials, agricultural by-products appear to be promising (from economic and environmental point of view) precursors to produce porous carbons, due of their low price and availability [26 - 32].

There are many studies related to the utilization of various biomass by using it as precursor for synthesis of carbons with different properties [33, 34]. It was established that chemical characteristics of the lignocellulosic biomass precursors have significant impact on the formation of carbon porosity. The essential effect of lipids, proteins, hemicellulose, cellulose and lignin content in the raw biomass precursor, on the properties of the final carbon products has been discussed [35, 36].

Table 1. Lethal oral doses and allowable concentrations in water of Cd and Hg.

Toxic metal	Maximal Allowable Concentration
Cd	lethal oral dose for humans - 350 - 3500 mg
	drinking water - 1 μg L^{-1}
Hg	lethal oral dose for humans - 1g
	drinking water - 1 μg L^{-1}

The main stages of the thermochemical processing of the raw biomass materials have been studied in detail, whereas the influence of carbonization [37 - 39] and activation [40, 41] conditions on the characteristics of the final carbon product has been investigated. The appropriate choice of ligno-cellulosic biomass precursor and selection of activation procedure results in formation of nanocarbons with high surface area and well-developed porosity, which is prerequisite for their various applications, such as supercapacitor and battery production [42], hydrogen storage [43], catalysis [44, 45], etc.

Novel nanoporous bio-chars with well-developed mesoporous structure, derived from juice industry residues, are obtained by applying a new energy-saving treatment method. This research is part of a project that aims to expand the raw material base to produce high-quality nanocarbons, by including waste biomass from the processing of various fruits materials, which have not been utilized before. To fulfil this goal, the chemical composition and texture of the selected raw materials and the optimal processing conditions will be determined, which will lead to the formation of the desired porous texture and surface chemistry of the final product. An important task of the research is to determine the applicability of the obtained carbon adsorbent for the purification of water from toxic pollutants.

EXPERIMENTAL

Raw materials

Raw materials - cherry stones and dried fruit residue from aronia, wastes and by-products from juice production (provided by Vitanea Ltd., Plovdiv, Bulgaria) - are selected for precursors. The selection of raw materials with different chemical composition aims to obtain information about the effect of the composition on the properties of the produced carbons. The raw materials contain lipids, proteins, hemicellulose, cellulose and lignin, and their content have significant influence on the properties of the resulting carbon product.

Determination of content of lipids, proteins, hemicellulose, cellulose and lignin is performed as follows. Four fractions were separated:

- The first fraction (lipids), which is soluble in a toluene-ethanol (1:1) mixture, is separated after extraction from raw material with particle size below 0.25 mm by a toluene-ethanol (1:1) mixture in extraction vessel. Duration of raw material exposure to the solution is 60 min with permanent stirring. 5 g of sample is added to 50 mL of solution.

- The second fraction (proteins and hemicellulose) is separated by extraction of the residue from first step with 0.94 mol L^{-1} water solution of H_2SO_4.

- The third fraction (cellulose) is separated by extraction of the residue from the previous step by 13.5 mol L^{-1} water solution of H_2SO_4.

- The lipids are solubilized in the first extraction step, proteins and hemicellulose in the second step, and cellulose in the third step. Lignin remains as residual fraction after the third step.

Preparation of nanocarbons

The carbon samples are synthesized as follows by two-step procedure. The carbonization (step 1) is performed in nitrogen atmosphere at 873 K (0.5 h). High temperature hydro pyrolysis (step 2) of the resulting carbonizates (obtained by step 1) is carried out (1 h) at 973, 1023 or 1073 K for the cherry stones, and at 923, 973 or 1023 K for the dry residue of aronia, respectively. The samples are denoted as ACC_T (from cherry stones; T- temperature, K) and ACA_T (from aronia residue; T - temperature, K), respectively.

Determination of oxygen-containing surface groups

Many properties of carbon materials, particularly their adsorption behaviour, are decisively influenced by chemisorbed oxygen. Oxygen in the surface oxides can be bound in the form of various functional groups. Surface oxides, formed by binding oxygen at elevated temperatures (or by aging) or with liquid oxidants, are acidic in character and they cause cation exchange properties. Acidic and basic surface sites coexist usually, but the concentration of basic sites decreases with increasing acidic character of the surface.

The acidic surface properties are caused by the presence of carboxyl groups (also in the form of their cyclic anhydrides), lactones or lactols, hydroxyl and phenolic groups.

The amount of surface oxygen-containing acidic functional groups is determined using Boehm method by neutralization with aqueous solutions of bases with increasing strength: $NaHCO_3$, Na_2CO_3, NaOH and sodium ethoxide [46]. It is accepted that $NaHCO_3$ can neutralize all carboxylic groups, Na_2CO_3 - carboxylic and lactonic groups, NaOH - carboxylic, lactonic and phenolic groups, and sodium ethoxide is assumed to neutralize all acidic groups. The total number of basic sites is determined by titration with HCl solution.

Nanotexture of the carbon adsorbents

The texture of bio-chars is characterized by N_2 (Porosimeter Quantachrome Autosorb iQ-C-XR-MP) adsorption isotherms at - 196°C. Before the experiments, the samples are outgassed under vacuum at 300°C. The specific surface area is evaluated from Brunauer-Emmett-Teller (BET) equation [47, 48], the total pore volume is determined at relative pressure 0.99, the micropore volume is calculated by V-t-method. The pores size distribution was calculated by DFT method [49].

Elemental analysis

Elemental analysis (C, H, N, and S) is carried out by Elementar Vario MACRO cube analyser (GmbH, Langenselbold, Germany). The amount of oxygen in the sample is calculated by the difference. The sum of carbon, hydrogen, nitrogen and sulfur content is subtracted from 100 %, and the result is the oxygen content.

Scanning electron microscopy (SEM)

The surface morphology is studied by high resolution

environmental scanning electron microscope JEOL JSM-6390 (Japan).

Iodine number

The iodine number (Standard No ASTM D4607-94) indicates the porosity and surface area of the activated carbon, and it is defined as the amount (mg) of iodine adsorbed by 1 g of carbon. The iodine adsorption was determined using the sodium thiosulfate volumetric method.

Cadmium adsorption experiments

100 mL stock solution (1 g L^{-1}) of cadmium (Cd^{2+}) standard is prepared by dissolving 0.2282 g cadmium sulfate $3CdSO_4.8H_2O$ (Merck) in distilled water. Diluted standard solutions were prepared from the stock solution with distilled water in different concentrations (25 - 100 mg L^{-1}). The adsorption capacity of the prepared carbon samples is investigated using aqueous solution of the cadmium in the range 25 - 100 mg L^{-1}. Batch adsorption studies are conducted at pH 5.5 - 6.1 in conical flasks, containing 10 mg carbon adsorbent and 50 mL Cd (II) solution with the desired concentration. Stopped flasks containing the adsorbent and the adsorbate with different concentration are agitated for predetermined intervals, using mechanical shaker at room temperature. After that the suspensions are filtered with microporous filter paper.

The amount of the Cd (II) ions in the solutions is determined spectrophotometrically by Pharo 300 UV-VIS Spectrophotometer. Alizarin Red S dye is used to form green coloured cadmium organic complex (detected at 422 nm) in the presence of Cd (II). The stoichiometric composition of the complex is 1:50 (Cd : Alizarin Red S). pH was adjusted using 0.1 M sodium hydroxide and 0.1 M hydrochloric acid [24].

Mercury adsorption experiments

The adsorption capacity of the carbon adsorbents for mercury was determined by the following procedure: 10 mg of the carbon was added to 50 mL of the aqueous solution of the $HgCl_2$ with different concentrations - from 25 to 100 mg L^{-1}.

The initial and equilibrium concentrations of the mercury in the solution were determined spectrophotometrically by Pharo 300 UV-Vis Spectrophotometer with rhodamine 6G [25].

The effect of pH on Hg (II) removal was studied using 0.01 g of carbon and 20 mg L^{-1} $HgCl_2$. The pH is adjusted by HCl or NaOH solutions.

pH determination

4.0 g carbon sample is immersed in 250 mL beaker and 100 mL distilled water is added. The beaker is covered with watch glass and heated up to 100°C. The supernatant liquid is poured off at 60°C. The decanted portion is cooled down to 25°C, and the pH is measured using pH meter JENWAY 3310 (Standard NORIT).

Point of zero charge (PZC)

The nature of carbon surface can be characterized by point zero charge (PZC) - the pH value, when the surface density of positive charges is equal to surface density of negative charges. The sample is immersed in appropriate volume of distilled water, and the mixture is stirred till equilibrium conditions (48 h). When equilibrium is reached, the pH value is measured. The plateau in the plot of equilibrium pH versus solid fraction amount corresponds to PZC value of the sample [27].

RESULTS AND DISCUSSION

Characterization of raw materials

Table 2 demonstrates a significant difference in the chemical composition of the selected raw materials. The results for aronia residue, in comparison with cherry stones, show higher lipid and lignin content, slightly lower cellulose content and lower hemicellulose content. After thermal treatment of the precursors, a significant change in the properties of the final products can be expected, according to a previous study [37]. Data shown in Table 3 confirm our expectations. As a result of carbonization of dried aronia residue, high amount of solid product is obtained. This effect could be due to the high content of lignin in this raw material. Predominantly aromatic structure of lignin provides high stability during the thermal treatment, which results in formation of higher amount of solid residue, as compared to solid residue from hemicellulose and cellulose [37]. The low amount of liquid and gas products released during thermal treatment of dried aronia residue is most probably due to considerably lower content of hemicellulose and cellulose in this precursor.

Nanocarbon characterization

The results for iodine adsorption and final product

Table 2. Chemical composition of the precursors.

Sample	Lipids, %	Hemicellulose and proteins, %	Cellulose, %	Lignin, %
Cherry stones	7.1	26.9	28.0	38.0
Aronia dry residue	36.0	10.2	3.1	50.7

Table 3. Material balance of the carbonization process at 873 K.

Sample	Solid products, %	Liquid products, %	Gaseous products, %
Cherry stones	23.75	31.50	44.75
Aronia dry residue	29.04	23.51	47.45

Table 4. Different characteristics of obtained bio-chars.

Sample	Raw material	Activation Temperature, K	Iodine number, mg g^{-1}	Carbon yield, wt. %
ACC_973	Cherry stones	973	850	19
ACC_1023	Cherry stones	1023	968	15
ACC_1073	Cherry stones	1073	1078	9
ACA_923	Dried aronia residue	923	555	21
ACA_973	Dried aronia residue	973	685	17
ACA_1023	Dried aronia residue	1023	750	10

Table 5. Main textural parameters of the obtained bio-chars from N_2 adsorption isotherms at 77 K.

Sample	Specific Surface Area S_{BET}, $m^2 g^{-1}$	Total Pore Volume V_{total}, $cm^3 g^{-1}$	Micropore Volume V_{micro}, $cm^3 g^{-1}$	Mesopore Volume V_{meso}, $cm^3 g^{-1}$
ACC	1083	1.40	0.16	1.23
ACA	561	0.37	0.23	0.14

yields of series of carbon samples are shown in Table 4. On the base of these results, the activation temperature was optimized to obtain nanocarbons with high yield and moderately high iodine capacity - 1023 K for activation of carbonizate from cherry stones, and 973 K for dried aronia residue carbonizate. Thus the samples ACC_1023 and ACA_973 are selected as most suitable for further experiments, and they will be denoted as ACC and ACA, respectively.

Fig. 1 and Table 5 present data from nitrogen physisorption experiments at 77 K. The isotherm of ACC (Fig. 1a) belongs to II type, according to IUPAC classification in the low-pressure region, indicating presence of micropores. However, at high pressure the isotherm could be attributed to IV type (IUPAC classification), typical for mesoporous materials. The

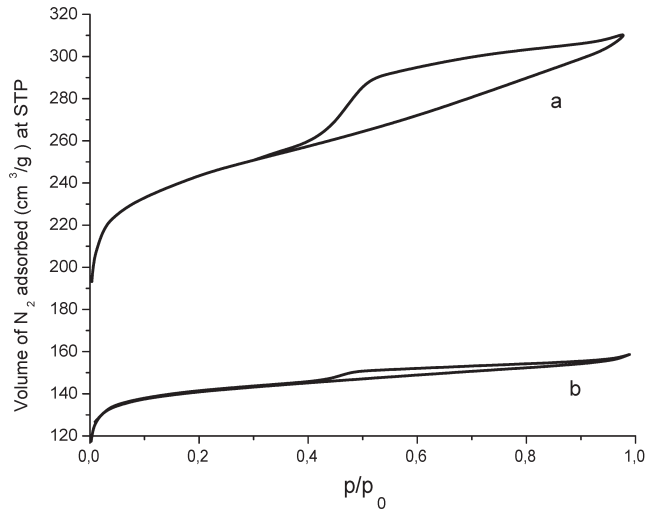

Fig. 1. N_2 adsorption isotherms at 77 K of bio-chars from cherry stones (a) and aronia waste (b).

complex course of the isotherm is related to combination of different adsorption mechanisms - surface coverage and pore condensation. The visible rounded knee indicates the approximate location of monolayer formation.

Low slope region in the middle of isotherm indicates the first few multilayers. The presence of hysteresis in the isotherm evidences capillary condensation in the meso- and macro-pores. Its appearance at around p/p0~0.4 indicates dominant presence of small mesopores. The co-existence of significant amount of micropores (pore diameter of 1 - 2 nm) and smaller mesopores (pore diameter of about 2 - 4 nm) is illustrated in Fig. 1.

The isotherm of ACA (Fig. 1b) belongs to I type (IUPAC classification), with steep initial region, due to very strong capillary condensation in the micropores. Fig. 1b show presence of micropores in the range 1.5 - 2.0 nm and small mesopores in the range 2.0 - 3.0 nm. In comparison with ACA, ACC sample possesses higher surface area, higher total pore volume and mesopore volume, and slightly lower micropore volume (Table 5). This is due to the differences in the chemical composition (lignin and cellulose content) of the precursors, and to the activation conditions. The presence of kernel in cherry stones and higher activation temperature used in this case could be responsible for development of wide mesoporosity in the final carbon product, because of diffusion of volatiles from the kernel, released during thermal treatment, through the hard cherry stones. Just the opposite, the texture of the carbon obtained from aronia char is not dense, which provides intensive burn-off processes with the temperature increase, and subsequent formation of carbon with high microporosity.

The results evidence significant difference in the textural parameters of bio-chars. In comparison with ACA, ACC sample possesses higher surface area, high total pore volume and mesopore volume, relatively smaller volume of micropores and higher average pore diameter. This is due to the difference in the chemical composition (lignin and cellulose content) of the precursors, as well as to activation conditions.

SEM results (Figs. 2 and 3) demonstrate that bio-char from cherry stone is distinguished by particles and pores of bigger size than these in the case of bio-char from aronia waste. Well distinguished Cd particles can be seen in SEM pictures of Cd-loaded bio-chars.

Oxygen-containing functional groups on the surface, which have different chemical features, are also determined. In case of bio-char obtained from cherry stones, big quantities of lactone and phenolic hydroxyl groups are present, whereas for the bio-char from aronia a large amount of carbonyl groups is detected (Table 6). The content of the oxygen-containing surface functional groups with basic character is similar for both samples.

Adsorption of Cd (II) ions

Kinetic study

The kinetic curves in Fig. 4 show the adsorption of Cd^{2+} on the synthesized activated carbons from solution with concentrations of 30 mg L^{-1}. Cd^{2+} adsorption increases sharply at a short contact time. The adsorption

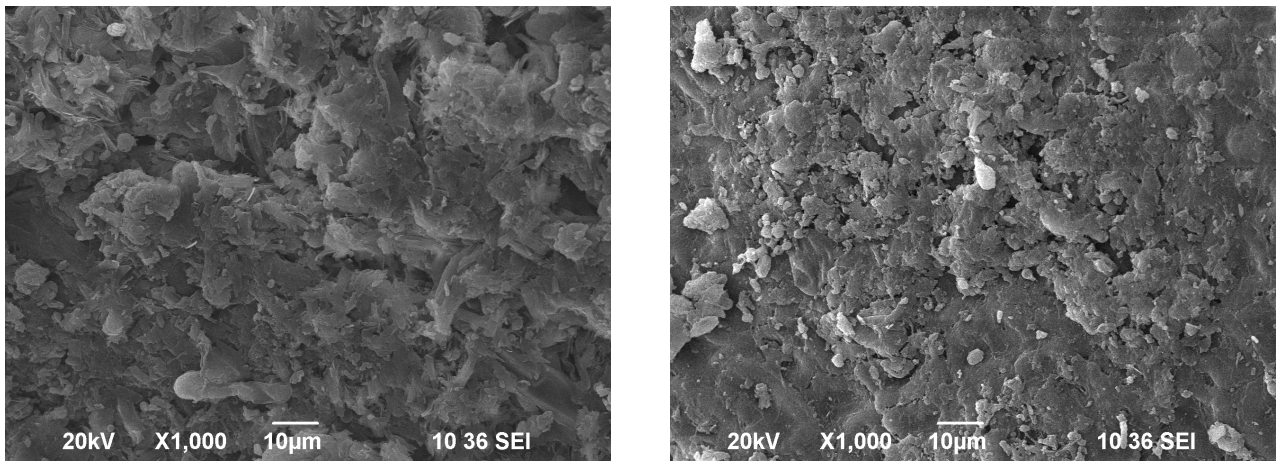

Fig. 2. SEM pictures of bio-char from cherry stone (a), Cd loaded bio-char from cherry stone (b).

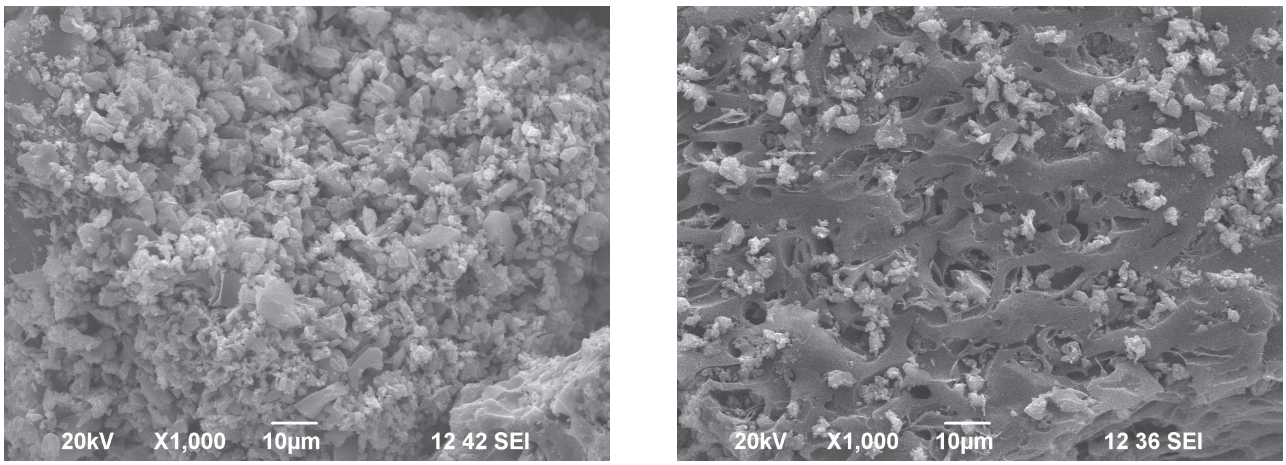

Fig. 3. SEM pictures of bio-chars from aronia waste (c), Cd loaded bio-char from aronia waste (d).

Table 6. Nature of the oxygen-containing functional groups on surface of the prepared carbons, obtained by Boehm titration.

Sample	Acidic groups, mmol g^{-1}				Total basic groups, mmol g^{-1}	pH	PZC
	Carboxylic	Lactone	Phenolic Hydroxyl	Carbonyl			
ACA	BDL	BDL	0.03	4.47	1.65	8.1	7.9
ACC	BDL	0.18	0.37	3.85	1.60	8.9	8.5

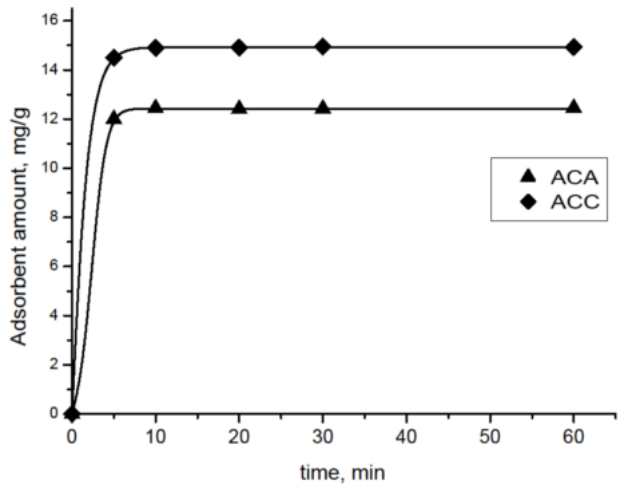

Fig. 4. Effect of treatment time and initial Cd^{2+} concentration on the adsorption of Cd^{2+}. Conditions: activated carbons amount, 10 mg / 50 mL; Cd^{2+} concentration: 30 mg L^{-1}.

process is quite fast and efficiently illustrates that the adsorption of Cd^{2+} is completed almost on the whole surface of activated carbons.

Furthermore, the adsorption capacity increases slowly, and the adsorption equilibrium is established within 10 min. The removal curves are smooth and continuous, leading to saturation, suggesting the possibility of formation of monolayer coverage of Cd^{2+} on the surface of the adsorbents. However, the low concentration of functional groups and the saturation of the available adsorption centers cause slow adsorption process.

Langmuir isotherm

The adsorption experimental data fit very well to the Langmuir isotherm model (Fig. 5). The linear form of the Langmuir Eq. (1) is given as:

$$Ce/qe = 1/(Qob) + Ce/Qo \quad (1)$$

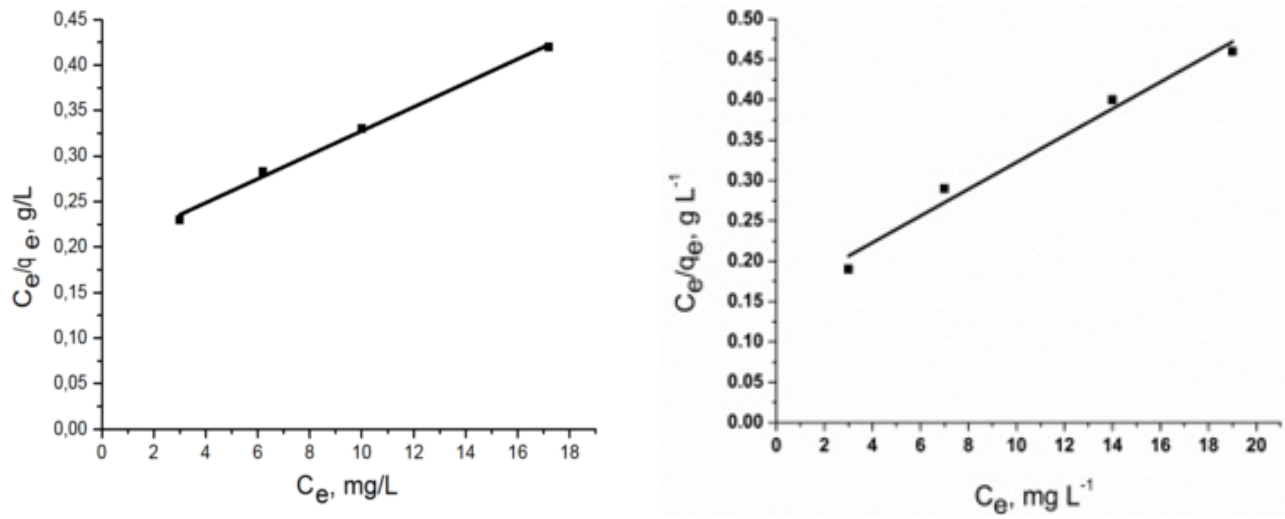

Fig. 5. Equilibrium adsorption isotherms of Cd^{2+} on ACC (a) and ACA (b). Conditions: adsorbent amount 10 mg / 50 mL solution, concentration 25 - 100mg L^{-1}, time of treatment 60 min, 25°C.

where C_e is equilibrium concentration (mg L^{-1}), q_e is the amount of Cd^{2+} adsorbed at equilibrium (mg g^{-1}), and Q_o (mg g^{-1}) and b (L mg^{-1}) are Langmuir constants, related to adsorption capacity and energy of adsorption, respectively. The values of Q_o and b are presented in Table 7.

The adsorption capacities (confirmed by atomic adsorption of the samples after cadmium removal) of cherry bio-char and aronia bio-char are 93 and 70 mg g^{-1}, respectively. These results are among the highest adsorption capacities found in the literature [1, 2].

Generally, the metal ion adsorption is determined by many factors, and the most significant of them are: ionic potential z/r (z is the ionic charge, i.e. oxidation ion state; r is the ionic radius, Å), chemical properties, ionic radius and hydrolysis process. Cadmium has relatively low ionic potential (1.9) as compared to other metal ions - for example 3.3 for lead, 2.8 for copper and 2.4 for zinc. Data for the pore size distribution of the carbons in Fig. 1 indicate that cadmium ions, with ionic radius (together with hydratiton shell) of 0.426 nm, according to Nightingale [50] can penetrate these micropores, e.g. the whole surface area of the carbons should be accessible for them.

Data for cadmium adsorption (Table 7) reveal that bio-char from cherry stones adsorbs larger amount of cadmium ions from an aqueous solution than bio-char from aronia. This could be due to better developed pore structure, greater number of mesopores with larger size, and significantly higher surface area of ACC (Table 5, Fig. 1a).

Table 7. Data for cadmium adsorption obtained from Langmuir plots.

Sample	Q_o, mg g^{-1}	b, L mg^{-1}	R^2 regression coefficient
ACC	93	0.061	0.986
ACA	70	0.014	0.984

Obviously, these factors are a prerequisite for easier access of cadmium ions to the surface of bio-char from cherry stones and determine its higher ability to remove cadmium ions from aquatic solution. The presence of more acidic oxygen groups (Table 6), which provides higher ion exchange capacity, also contributes to larger adsorption of cadmium ions on the surface of carbon from cherry stones. The investigation demonstrates that obtained nanocarbons are appropriate for removal of cadmium ions from aqueous solutions.

Studying the effect of pH of the external solution on the extent of adsorption on carbons is important for understanding the adsorption process (Fig. 6). It is evident that at pH 2.5 - 4.5 the percentage removal increases sharply, and at higher pH values saturation is attained.

Adsorption process depends on the nature of the adsorbent surface, and especially on the content of

different oxygen groups and on the charge of the surface. At low pH values (Fig. 6) there is electrostatic repulsion between ions and the positively charged carbon surface. Besides, the H^+ ions, which are available in high concentrations at lower pH of the solution, compete with the positively charged Cd (II) ions for the adsorption sites, thus hindering the adsorption of cadmium.

It is well known that the oxygen-containing functional groups on the carbons surface play an important role in metal adsorption. In our study presence of acidic groups - phenolic/hydroxyl and carbonyl, as well as basic groups were detected on the carbon surface.

Cd adsorption (cadmium loading, 7 and 9 %, respectively, of the carbon samples is confirmed by atomic adsorption) most probably include formation of surface complexes with the participation of the functional groups on the surface of carbon. The following possible reactions and adsorption mechanism are proposed (Eq. (2), Eq. (3)):

$$CxOH^{2+}\ (surface) + Cd^{2+} \text{ “ } CxOCd^{2+}\ (adsorbed) + 2H^{+} \quad (2)$$

$$2CxOH^{+}\ (surface) + Cd^{2+} \text{”} (CxO)_2Cd^{2+}\ (adsorbed) + 2H^{+} \quad (3)$$

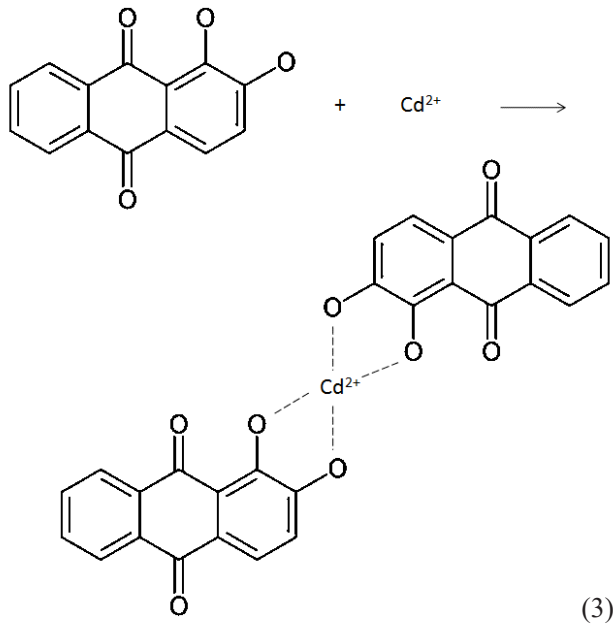

(3)

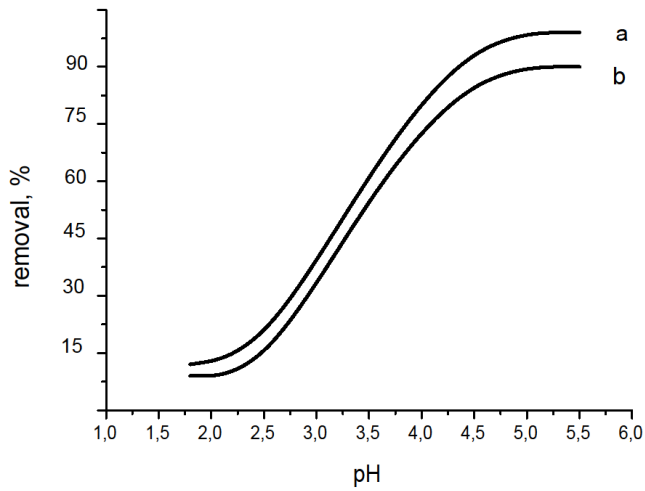

Fig. 6. Effect of pH on cadmium removal on carbons derived from cherry stones (a) and aronia residue (b). Conditions: time of treatment - 60 min, activated carbon amount - 10 mg/50 mL, Cd^{2+} concentration - 80 mg L^{-1}, 25°C.

Metal ion adsorption is determined by many factors: ionic potential z/r (z is the ionic charge, i.e. oxidation ion state; r is the ionic radius, Å), chemical properties, ionic radius and hydrolysis process.

Cadmium has relatively low ionic potential (1.9) as compared to other metal ions - for example 3.3 for lead, 2.8 for copper and 2.4 for zinc.

Data for cadmium adsorption reveal that carbon from cherry stones adsorbs higher amount of cadmium ions from an aqueous solution than the nanocarbon from aronia residue. This could be due to more developed pore structure, higher number of mesopores with bigger size, and significantly higher surface area of ACC.

The presence of more acidic oxygen groups which provides higher ion exchange capacity, also contributes to higher degree of adsorption of cadmium ions on the surface of bio-char from cherry stones. The investigation demonstrates that obtained nanoporous bio-chars are appropriate for removal of cadmium ions from aqueous solutions.

Adsorption of Hg (II) ions

Adsorption kinetics

The kinetic curves of Hg (II) adsorption on the synthesized adsorbents from a solution with a metal concentration of 30 mg L^{-1} have a similar profile to the

kinetic curves of Cd (II) adsorption. The adsorption of metal ions increases sharply with a short contact time. The adsorption process is quite fast and efficient, indicating that the adsorption of metal ions occurs almost on the entire surface of the activated carbon. Then, the adsorption capacity increases slowly, and the adsorption equilibrium is established within 20 min. The removal curves are smooth and continuous, leading to saturation, which suggests the possibility of the formation of a monolayer coating of Hg (II) on the adsorbent surface. However, since the limited functional groups and the saturation of relatively less available adsorption sites may affect the slowing down of the adsorption process. Considering the practical work, the optimal contact time was chosen to be 20 min for further adsorption experiments.

Langmuir isotherm

Some theoretical parameters in the Langmuir equation were calculated from the experimental data, and they are presented in Table 8. The surface area covered by Hg (II) ions was calculated based on the Goldschmidt ionic radius of 0.112 nm. From the data obtained from Langmuir isotherms, it is shown that there is a similarity between the two adsorptions of Hg and Cd. Again, it can be assumed that the higher adsorption of activated carbon obtained from cherry stones is due to a better developed pore structure, a greater number of mesopores with a larger size, and a higher amount of acidic oxygen groups (Table 8, Fig. 7 a, b and Table 6).

In the case of mercury (II) solutions, most of the mercury exists in the form of complexes, which can be positive, neutral or negative, depending on the composition and pH of the solution. Appropriate amounts of hydrochloric acid and sodium hydroxide are added to obtain a solution with different pH values. The adsorption capacity of the carbon was investigated at different pH values, and a maximum was found near pH 6.0 for all samples. The metal uptake increased in the pH range from 2 to 5.5 and remained constant above pH 6 for all carbons. The effect of the solution on the adsorption of mercury ions for the samples studied is illustrated in Fig. 8 (for an initial concentration of

Table 8. Data for Hg (II) adsorption obtained from Langmuir plots.

Sample	Q_o, mg g^{-1}	b, L mg^{-1}	R^2 regression coefficient
ACC	104	0.816	0.964
ACA	83	0.065	0.985

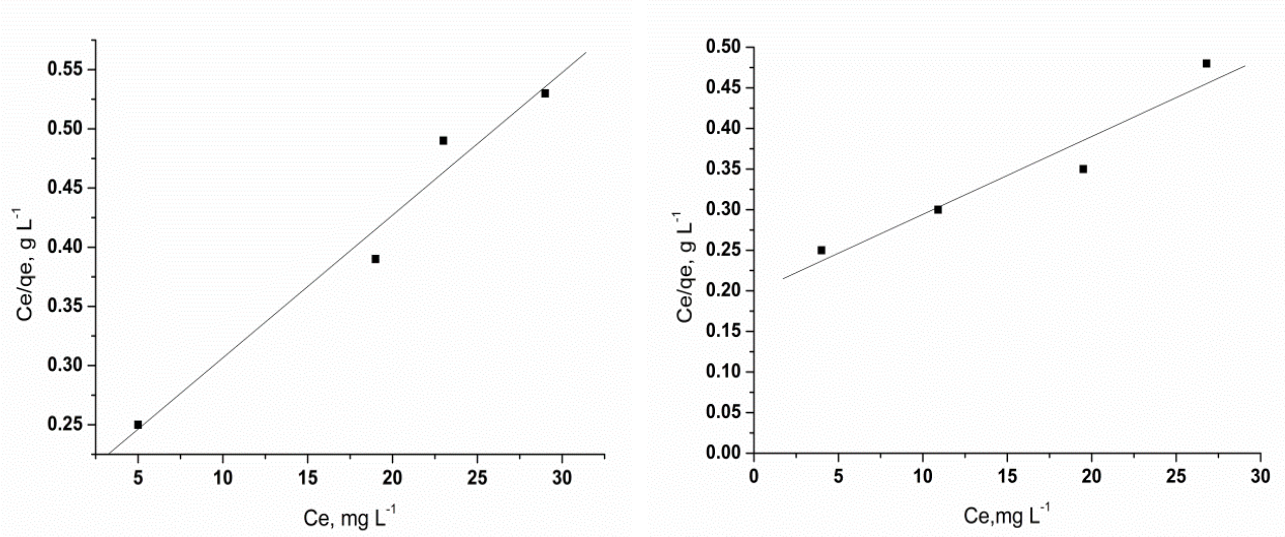

Fig. 7. Equilibrium adsorption isotherms of Hg^{2+} on ACC (a) and ACA (b). Conditions: adsorbent amount 10 mg/50 mL solution, concentration 25 - 100 mg L^{-1}, time of treatment 60 min, 25°C.

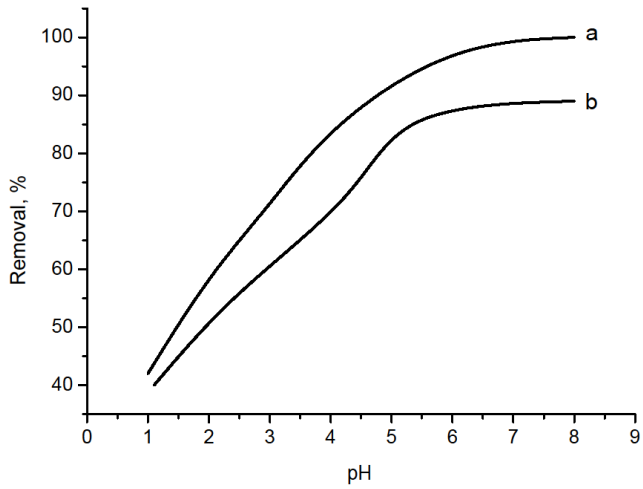

Fig. 8. Effect of pH on mercury removal on carbons derived from cherry stones (a) and aronia residue (b). Conditions: time of treatment - 60 min, activated carbon amount-10 mg/50 mL, Hg^{2+} concentration - 80 mg L^{-1}, 25°C.

80 mg L^{-1}). Considering that activated carbon A has a larger pore volume and total surface area than carbon B, it is obvious that the removal efficiency is not directly related to these quantities. However, this may be related to differences in the pore size distribution and surface chemistry of the carbon. It can be shown by stability constant calculations that in the presence of Cl^- the predominant species at pH > 4.0 is $Hg(OH)_2$, and at pH < 4 the predominant species is $HgCl_2$. The dominant species in the range of highest sorption efficiency is $Hg(OH)_2$. When the pH decreases, various chloride species appear, especially $HgCl_2$ (aq), which are poorly adsorbed. It is assumed that in addition to the various oxygen-containing groups, $CxSO_3H$ groups are present on the carbon surface because of the participation of H_2SO_4 in the process of obtaining activated carbon. The complexes described in the Eq. (4) - Eq. (6) are most probably formed:

$$2CxOH + Hg^{2+} \rightarrow (CxO)Hg^{2+} + 2H^{+} \quad (4)$$

$$2CxOOH + Hg^{2+} \rightarrow (CxCOO)2Hg^{2+} + 2H^{+} \quad (5)$$

$$2CxSO_3H + Hg^{2+} \rightarrow (CxSO_3)Hg^{2+} + 2H^{+} \quad (6)$$

The values of maximal adsorption capacity for our samples are much higher than the literature data for adsorption of mercury and cadmium, reported by other researchers (Table 9).

Regeneration of carbon adsorbents after Cd adsorption

The Cd^{2+} loaded bio-chars (5 g each) were mixed with portions of 50 mL of 20 % HCl solution and the mixtures is left at 60°C for 1 h. The suspensions were then filtered and further portions of 50 mL of NaOH solutions are added and stirred for 1h, then filtered again and dried at 60°C for 8 h. The results show that treatment with HCl leads to 90 % regeneration of both activated carbons. The degree of regeneration was estimated by determining the adsorption capacities obtained by iodine adsorption experiments before and after Cd^{2+} loading.

Regeneration of carbon adsorbents after Hg adsorption

The Hg^{2+} loaded bio-char (5 g each) were mixed with portions of 50 mL of 10 % KI solution and the mixtures is left at 60°C for 1 h. The suspensions were then filtered

Table 9. Monolayer adsorption capacity of mercury and cadmium in various adsorbents obtained from Langmuir model.

Metal	Adsorbent type	qm, mg g^{-1}	Reference
Cd	Cherry stone	93.00	This study
	Aronia	70.00	This study
	Aluminum oxide	35.06	[51]
	Rape straw	73.30	[52]
	Olive stone	10.44	[53]
Hg	Cherry stone	104.00	This study
	Aronia	83.00	This study
	Bagasse biochar	13.00	[54]
	Hickory chips biochar	5.00	[54]
	Wood chip activated carbon	2.00	[54]

and dried at 60°C for 8 h. The results show that treatment with KI leads to 90 % regeneration of both bio-char. The degree of regeneration was estimated by determining the adsorption capacities obtained by iodine adsorption experiments before and after Hg^{2+} loading.

CONCLUSIONS

To perform recovery of wastes from the industry and agriculture, together with purification of waters from different pollutants, as well as to find efficient energy sources without environmentally harmful impact, a suitable treatment method was developed and applied. This new treatment method converts waste biomass from the juice industry (cherry stones and dry residue from aronia) to high-grade nanocarbons, distinguished by well-developed porous structure and tunable surface chemistry, and with potential application for environmental protection.

It was established that physico-chemical properties of the obtained carbons depend on the composition and the plant texture of the corresponding raw materials. Precursors with considerably high content of cellulose, hemicellulose, and lignin (cherry stones) lead to formation of carbons containing micro- and mesopores, while the raw materials with a higher content of lipids and lignin (dried fruit residue of aronia) yield carbon with narrow microporosity.

The adsorption capacities of cherry bio-char and aronia bio-char are 93 and 70 mg g^{-1}, for Cd (II) removal, and 83 and 104 mg g^{-1}, for Hg (II) respectively.

The obtained nanocarbons, particularly the carbons from cherry stones, are appropriate for removal of highly toxic cadmium and mercury ions from waste waters. The adsorption capacity of carbon adsorbent towards both metal ions is determined by the carbon porous structure, pore size and chemical nature of the surface.

The obtained bio-chars are suitable for removal of heavy metal ions from aqueous solution. In further investigations with real waste waters are planned. The extent of removal of metal ions is determined by the porous structure of the carbon, pore size and chemical nature of the surface.

Acknowledgments

The authors acknowledge financial support for this work by the Bulgarian National Science Fund, grant number KP-06-M77/2. This research was funded supported by the Grant Project №BG16RFPR002-1.014-0015: "Clean Technologies for Sustainable Environment - Water, Waste, Energy for Circular Economy", financed by the European Regional Development Fund through Bulgarian Programme "Research, Innovation and Digitalisation for Smart Transformation". The authors are also grateful to the funding by Project BG-RRP-2.017-0006 from Recovery Plan for Europe (NextGenerationEU) and appreciate the support from Romanian-Bulgarian Academia Joint Project INNOMAG.

Authors' contributions

Conceptualization, I.S., B.P., P.D., N.P. and B.Ts.; methodology, I.S., B.P., N.P., B.Ts., G.T., A.K., M.A., T.S. and A.S.; investigation, I.S., B.P., N.P., B.Ts., G.T., M.A., A.K., T.S. and A.S.; writing - original draft preparation, I.S., B.P., N.P., B.Ts., A.S., T.S., P.D. ; writing - review and editing, I.S.,B.P., N.P., B.Ts., A.S., T. S., P.D..; supervision, I.S., B.P., N.P., B. Ts., T.S., P.D.; project administration, I.S., B. Ts., T.S.,P.D. funding acquisition, I.S., B. Ts., T.S., N.P., P.D. All authors have read and agreed to the published version of the manuscript.

REFERENCES

1. K. Bhattacharyya, D. Sen, A. Kumar Banik, S. Ganguly, Adsorptive removal of cadmium from aqueous medium-a critical review, Phys. Chem. Earth, 134, 2024, 103538. https://doi.org/10.1016/j.pce.2023.103538.
2. Z. Yanfeng, L. Huageng, Y. Ruilian, H. Gongren, C. Fu, Removal of Aquatic Cadmium Ions Using Thiourea Modified Poplar Biochar, Water, 12, 4, 2020, 1117. https://doi.org/10.3390/w12041117.
3. E.P. Puglla, D. Guaya, C. Tituana, F. Osorio, M.J. Garcia-Ruiz, Biochar from Agricultural by-products for the Removal of Lead and Cadmium from Drinking Water, Biochar from Agricultural by-products for the Removal of Lead and Cadmium from Drinking Water, Water, 12, 10, 2020, 2933. https://doi.org/10.3390/w12102933.
4. F. Chen, Y. Sun, C. Liang, T. Yang, S. Mi, Y. Dai, M. Yu, Q. Yao, Adsorption characteristics and

mechanisms of Cd^{2+} from aqueous solution by biochar derived from corn stover, Sci. Rep., 12, 1, 2022, 17714. https://doi.org/10.1038/s41598-022-22714-y.

5. R.Z. Wang, D.L. Huang, Y.G. Liu, C. Zhang, C. Lai, G.M. Zeng, M. Cheng, X.M. Gong, J. Wan, H. Luo, Investigating the adsorption behavior and the relative distribution of Cd^{2+} sorption mechanisms on biochars by different feedstock, Bioresour. Technol., 261, 2018, 265-271. https://doi.org/10.1016/j.biortech.2018.04.032.
6. K. Pyrzynska, Removal of cadmium from wastewaters with low-cost adsorbents, J. Environ. Chem. Eng., 7, 1, 2019, 102795. https://doi.org/10.1016/j.jece.2018.11.040**.**
7. S. Hydari, H. Sharififard, M. Nabavinia, M.R. Parvizi, A comparative investigation on removal performances of commercial activated carbon, chitosan biosorbent and chitosan/activated carbon composite for cadmium, Chem. Eng. J., 193–194, 2012, 276-282. https://doi.org/10.1016/j.cej.2012.04.057.
8. I. Osasona, K. Aiyedatiwa, J.A. Johnson, O.L. Faboya, Activated carbon from spent brewery barley husks for cadmium ion adsorption from aqueous solution, Indones. J. Chem., 18, 2018, 145-152. https://doi.org/10.22146/ijc.22422.
9. U.I. Gaya, E. Otene, A.H. Abdullah, Adsorption of aqueous Cd (II) and Pb (II) on activated carbon nanopores prepared by chemical activation of doum palm shell, SpringerPlus, 4, 2015, 458. https://doi.org/10.1186/s40064-015-1256-4.
10. M. Fronczak, K. Pyrzynska,A. Bhattarai, P. Pietrowski, M. Bystrzejewski, Improved adsorption performance of activated carbon covalently functionalised with sulphur-containing ligands in the removal of cadmium from aqueous solutions, Int. J. Environ. Sci. Technol. 16, 2019, 7921-7932. https://doi.org/10.1007/s13762-019-02398-0.
11. R. Dhahri, M. Yılmaz, L. Mechi, A. Khalaf, D. Alsukaibi, F. Alimi, Y. Moussaoui, Optimization of the Preparation of Activated Carbon from Prickly Pear Seed Cake for the Removal of Lead and Cadmium Ions from Aqueous Solution, Sustainability 14, 6, 2022, 3245. https://doi.org/10.3390/su14063245.
12. G. Bhanjana, N. Dilbaghi, K.-H. Kim, S. Kumar, Carbon nanotubes as sorbent material for removal of cadmium, J. Mol. Liq., 242, 2017, 966-970. https://doi.org/10.1016/j.molliq.2017.07.072.
13. W. Hao, T. Kashiwabara, R. Jin, Y. Takahashi, M. Gingras, D.S. Alessi, K.O. Konhauser, Clay minerals as a source of cadmium to estuaries, Sci. Rep., 10, 2020, 1-11. https://doi.org/10.1038/s41598-020-67279-w.
14. W. Zhou, L. Ren, L. Zhu, Reducement of cadmium adsorption on clay minerals by the presence of dissolved organic matter from animal manure, Environ. Pollut., 223, 2017, 247-254. https://doi.org/10.1016/j.envpol.2017.01.019.
15. M.H. Ehrampoush, M. Miria, M.H. Salmani, A.H. Mahvi, Cadmium removal from aqueous solution by green synthesis iron oxide nanoparticles with tangerine peel extract, J. Environ. Heal. Sci. Eng., 13, 2015, 1-7. https://doi.org/10.1186/s40201-015-0237-4.
16. Y. Sun, S. Zhou, P.C. Chiang, K.J. Shah, Evaluation and optimization of enhanced coagulation process: Water-Energy Nexus, 2, 1, 2019, 25. https://doi.org/10.1016/j. wen.2020.01.001.
17. K.C. Khulbe, T. Matsuura, Removal of heavy metals and pollutants by membrane adsorption techniques, Appl. Water Sci., 8, 2018, 19. https://doi.org/10.1007/s13201-018-0661-6.
18. C.M. Simonescu, V. Lavric, A. Musina, O.M. Antonescu,D.C. Culita, V. Marinescu, C. Tardei, O. Oprea, Pandele, A.M. Experimental and modeling of cadmium ions removal by chelating resins, J. Mol. Liq., 307, 1, 2020, 112973. https://doi.org/10.1016/j.molliq.2020.112973.
19. G. Hilsion, Abatement of mercury pollution in the small-scale gold mining industry: Restructuring the policy and research agendas, Sci. Total Environ., 362, 2006, 1-14. https://doi.org/10.1016/j.scitotenv.2005.09.065
20. F. Di Natale, A. Lancia, A. Molino, M. Di Natale, D. Karatza, D. Musmarra, Capture of mercury ions by natural and industrial materials, J. Hazard. Mater., 132, 2006, 220-225. https://doi.org/10.1016/j.jhazmat.2005.09.046
21. A. Essa, L. Macaskie, N. Brown, A new method for mercury removal, Biotechnol. Lett., 27, 2005, 1649-1655. DOI 10.1007/s10529-005-2722-9
22. C.P. Nanseu-Njiki, S.R. Tchamango, P.C. Ngom, A.

Darchen, E. Ngameni, Mercury (II) removal from water by electrocoagulation using aluminium and iron electrodes, J. Hazard. Mater., 168, 2009, 1430-1436. doi: 10.1016/j.jhazmat.2009.03.042.

23. A.E. Putun, N. Ozba, E.P. Onal, E. Putun, Fixed-bed pyrolysis of cotton stalk for liquid and solid products, Fuel Process. Technol., 86, 2005, 1207-1219. https://doi.org/10.1016/j.fuproc.2004.12.006
24. Deswati, H. Pardi, S. Hamzar, Z. Rahmiana, Adsorptive Cathodic Stripping Voltammetric Method with Alizarin for the Simultaneous Determination of Cadmium, and Zinc in Water Samples, Orient. J. Chem., 32, 2016, 3071-3080. DOI:10.13005/ojc/320628T.V.
25. T.V. Ramakrishna, G. Aravamundan, M. Vijayakumar, Spectrometric determination of mercury (II) as the ternary complex with rhodamine and iodide, Anal. Chim Acta, 84, 1976, 369-375. DOI: 10.1016/S0003-2670(01)82236-4
26. G. Socrates, Infrared Charecteristic Group Frequencies, Wiley, New York, 1994.
27. J.S. Noh, J.A. Schwarz, Estimation of the Point of Zero Charge of Simple Oxides by Mass Titration, J. Colloid Interface Sci., 130 1989, 157-164. https://doi.org/10.1016/0021-9797(89)90086-6
28. K. Uddin, I.I. El-Sharkawy, T. Miyazaki, B.B. Saha, Sh. Koyama, H.S. Kil, J. Miyawaki, S.H. Yoon, Adsorption characteristics of ethanol onto functional activated carbons with controlled oxygen content, Appl. Therm. Eng., 72, 2014, 211-218. https://doi.org/10.1016/j.applthermaleng.2014.03.062
29. K. Uddin, I.I. El-Sharkawy, T. Miyazaki, B. Saha, Sh. Koyama, Thermodynamic analysis of adsorption cooling cycle using ethanol-surface treated Maxsorb III pairs, Evergreen, 1, 2014, 25-31. https://doi.org/10.5109/1440973
30. M.A. Yahya, Z. Al-Qodah, C.W. Z. Ngah, Agricultural bio-waste materials as potential sustainable precursors,used for activated carbon production, Renewable and Sustainable Energy Rev., 46, 2015, 218-235. https://doi.org/10.1016/j.rser.2015.02.051
31. N. Álvarez-Gutiérrez, M.V. Gil, F. Rubiera, C. Pevida, Kinetics of CO_2 adsorption on cherry stone-based carbons in CO_2/CH_4 separations, Chem. Eng. J., 307, 2017, 249-257. https://doi.org/10.1016/j.cej.2016.08.077
32. N.D. Martinez, R.B. Venturini, H.S. Silva, J.E. Gonzalez, A.M. Rodriguez, Copper on activated carbon for catalytic wet air oxidation, Mater. Res.,12, 1, 2009, 45-50. http://dx.doi.org/10.1590/S1516-14392009000100004
33. K.-W. Jung, B.H. Choi, M.J. Hwang, T.-U. Jeong, K.-H. Ahn, Fabrication of granular activated carbons derived from spent coffee grounds by entrapment in calcium alginate beads for adsorption of acid orange 7 and methylene blue, Bioresour. Technol., 219, 2016, 185-195. https://doi.org/10.1016/j.biortech.2016.07.098
34. O. Ioannidou, A. Zabaniotou, Agricultural residues as precursors for activated carbon production, Renewable and Sustainable Energy Rev., 11, 2007, 1966-2005. https://doi.org/10.1016/j.rser.2006.03.013
35. M.S. Islam, M.A. Rouf, Waste biomass as sources for activated carbon production - a review, Bangladesh J. Sci. Ind. Res., 47, 2012, 347-364. https://doi.org/10.3329/bjsir.v47i4.14064
36. C.R. Correa, T. Otto, A. Kruse, Influence of the biomass components on the pore formation of activated carbon, Biomass Bioenergy, 97, 2017, 53-64. https://doi.org/10.1016/j.biombioe.2016.12.017
37. B. Tsyntsarski, B. Petrova, T. Budinova, N. Petrov, Influence of the chemical composition of agricultural by-products on their behaviour during thermal treatment, Bulg. Chem. Commun., 38, 2006, 289-292. http://www.bcc.bas.bg/
38. G.B. Barin, I.F. Gimenez, L.P. da Costa, A.G.S. Filho, L.S. Barreto, Influence of hydrothermal carbonization on formation of curved graphite structures obtained from a lignocellulosic precursor, Carbon, 78, 2014, 609-612. https://doi.org/10.1016/j.carbon.2014.07.017
39. Zh. Li, W. Lv, Ch. Zhang, B. Li, F. Kang, Q.-H. Yang, A sheet-like porous carbon for high-rate supercapacitors produced by the carbonization of an eggplant, Carbon, 92, 2015, 11-14. https://doi.org/10.1016/j.carbon.2015.02.054
40. N. Álvarez-Gutiérrez, M.V. Gil, F. Rubiera, C. Pevida, Cherry-stones-based activated carbons as potential adsorbents for CO_2/CH_4 separation: effect of the activation parameters, Greenhouse Gases: Sci. Technol., 5, 2015, 812-825. https://doi.org/10.1002/ghg.1534

41. M. Song, B. Jin, R. Xiao, L. Yang, Yi. Wu, Zh. Zhong, Ya. Huang, The comparison of two activation techniques to prepare activated carbon from corn cob, Biomass Bioenergy, 48, 2013, 250-256. https://doi.org/10.1016/j.biombioe.2012.11.007
42. Q. Li, Yo. Zhu, P. Zhao, Ch. Yuan, M. Chen, Ch. Wang, Commercial activated carbon as a novel precursor of the amorphous carbon for high-performance sodium-ion batteries anode, Carbon, 129, 2018, 85-94. https://doi.org/10.1016/j.carbon.2017.12.008
43. G. Sethia, A. Sayari, Activated carbon with optimum pore size distribution for hydrogen storage, Carbon, 2016, 99, 289-294. https://doi.org/10.1016/j.carbon.2015.12.032
44. A. Barroso-Bogeat, M. Alexandre-Franco, C. Fernández-González, V. Gómez-Serrano, Preparation of activated carbon-metal oxide hybrid catalysts: textural characterization, Fuel Process. Technol., 126, 2014, 95-103. https://doi.org/10.1016/j.fuproc.2014.04.022
45. M.C. Pereira, F.S. Coelho, C.C. Nascentes, J.D. Fabris, M.H. Araujo, K. Sapag, L.C.A. Oliveira, R.M. Lago, Use of activated carbon as a reactive support to produce highly active-regenerable Fe-based reduction system for environmental remediation, Chemosphere, 2010, 7-12. https://doi.org/10.1016/j.chemosphere.2010.07.056
46. E. Papirer, Sh. Li, J.B. Donnet, Contribution to the study of basic surface groups on carbons, Carbon, 25, 1987, 243-247. https://doi.org/10.1016/0008-6223(87)90122-9
47. V. Gomez-Serrano, C. Gonzalez-Garcia, M. Gonzalez-Martin, Nitrogen adsorption isotherms on carbonaceous materials. Comparison of BET and Langmuir surface areas, Powder Technol., 116, 2001, 103-108. https://doi.org/10.1016/S0032-5910(00)00367-3
48. A.V. Neimark, P.I. Ravikovitch, M. Grun, F. Schuth, K. K. Unger, Characterization of Porous Solids IV , Bath, UK, Academic Press, 1996.
49. S.G. Chen, R.T. Yang, Theoretical basis for the potential theory adsorption isotherms: the Dubinin-Radushkevich and Dubinin-Astakhov equation, Langmuir 10, 1994, 4244-4249. https://doi.org/10.1021/la00023a054
50. E.R. Nightingale, Phenomenological Theory of Ion Solvation. Effective Radii of Hydrated Ions, J. Phys. Chem. 63, 1959, 1381-1387. https://doi.org/10.1021/j150579a011
51. T.K. Naiya, A.K. Bhattacharya, S.K. Das, Adsorption of Cd (II) and Pb (II) from aqueous solutions on activated alumina, J. Colloid Interface Sci., 333, 2009, 14-26. https://doi.org/10.1016/j.jcis.2009.01.003
52. Z. Zhang, T. Wang, H. Zhang, Y. Liu, B. Xing, Adsorption of Pb (II) and Cd (II) by magnetic activated carbon and its mechanism, Sci. Total Environ., 757, 2021, 143910. https://doi.org/10.1016/j.scitotenv.2020.143910
53. I. Kula,M. Uğurlu, H. Karaoğlu, Ali. Çelik, Adsorption of Cd(II) ions from aqueous solutions using activated carbon prepared from olive stone by $ZnCl_2$ activation, Bioresour. Technol., 99, 2008, 492-501. https://doi.org/10.1016/j.biortech.2007.01.015
54. X. Xu, A. Schierz, N. Xu, X. Cao, Comparison of the characteristics and mechanisms of Hg(II) sorption by biochars and activated carbon, J. Colloid Interface Sci., 463, 2016, 55-60. https://doi.org/10.1016/j.jcis.2015.10.003